Rare Metal Materials and Engineering
Volume 47, Issue 2, February 2018
Online English edition of the Chinese language journal

Available online at www.sciencedirect.com

ScienceDirect

Cite this article as: Rare Metal Materials and Engineering, 2018, 47(2): 0479-0484.

ARTICLE

Hardness and Modulus of Cu-based Bulk Metallic Glasses via Nanoindentation

Pi Jinhong, Wang Zhangzhong, He Xiancong, Bai Yunqiang

Jiangsu Key Laboratory of Advanced Structural Materials and Application Technology, Nanjing Institute of Technology, Nanjing 211167, China

Abstract: The hardness and Young'modulus for two Cu-based bulk metallic glasses, $Cu_{59}Zr_{36}Ti_5$ and $Cu_{61}Zr_{34}Ti_5$, has been studied by nanoindentation in three different ways, including load rate control mode, load control mode, and cycles load control mode. Young's modulus of the specimen shows the dependence on loading rate when the loading rate is no more than 5 mN/s. The Young's modulus of both $Cu_{59}Zr_{36}Ti_5$ and $Cu_{61}Zr_{34}Ti_5$ decreases with the increasing of holding load and loading rate. But neither loading rate nor holding load has significant influence on hardness. Cyclic loading leads to slight hardening for $Cu_{59}Zr_{36}Ti_5$, while $Cu_{61}Zr_{34}Ti_5$ doesn't show such results. What's more, $Cu_{61}Zr_{34}Ti_5$ exhibits obviously higher hardness and modulus than $Cu_{59}Zr_{36}Ti_5$.

Key words: nanoindentation; Cu-based bulk metallic glass; cycles load control; hardening

As a promising metallic material, bulk metallic glass (BMG) has attracted an increasing interest from not only pure scientific communities but also practices in engineering[1,2]. Thanks to its surprising mechanical properties, such as high fracture strength, super high elastic limit, and superior corrosion resistance, BMG has a great received potential to be used as an engineering material[3,4]. Among them, Cu-based bulk metallic glasses have received more and more attention in recent years, owing to their excellent performances, such as low production cost and relative high glass-forming ability[5,6]. However, practical engineering commercialization of BMGs are severely restricted due to their severely limited global plasticity when deformed at room temperature, as they tend to fail catastrophically along one dominant shear band of few tens of nanometers thickness[7,8]. And this shortcoming manifests as abrupt fractures resulting from shear band formation. Meanwhile, it should be noticed that it has been reported that certain BMGs (e.g., some Zr-, Pd-, Pt- or Cu-based ones) can exhibit values of plastic deformation around 20% or more when compressed at room temperature in recent years [9]. There are some intrinsic parameters that favor large plasticity and toughness, and the deformation mechanism in metallic glass is under debate [1], although impressively large values of plastic strains have been attributed to either nano scale phase separation or nanocrystallization by many researchers[9,10]. So, a thorough comprehension of the plastic deformation mechanism of BMGs is of great benefit to the development and design of strong and tough BMGs.

Nanoindentation has been performed in the past decades to study the deformation behavior of BMGs on a local scale and at varying deformation rates. Greer et al. observed that the load-displacement curves had staircase-like shapes at low deformation rates, which were related to the discrete activation of shear bands. At high loading rates smooth load-displacement curves were obtained, leading to the suggestion that homogeneous yielding might occur in this regime[10]. Haag et al. reported the effect of loading rates on the serrated flow of bulk metallic glass during nanoindentation and proposed that changes to flow serration did not represent a distinct physical phenomenon but rather the increasing irresolvability of displacement bursts[11]. Strain rate sensitivity of plastic flow in metallic

Received date: March 17, 2017
Foundation item: Open Fund of Jiangsu Key Laboratory of Advanced Structural Materials and Application Technology (ASMA201418); Innovation Fund (CKJA201301) and Dr. Special Found (ZKJ201403) of Nanjing Institute of Technology
Corresponding author: Pi Jinhong, Ph. D., Associate Professor, School of Materials Engineering, Nanjing Institute of Technology, Nanjing 211167, P. R. China, Tel: 0086-25-86118274, E-mail: pijinhong@njit.edu.cn

glasses has also been reported[12,13]. Obviously, nanoindentation has played an important role in BMGs.

In this paper, two Cu-based bulk metallic glasses, $Cu_{59}Zr_{36}Ti_5$ and $Cu_{61}Zr_{34}Ti_5$, were studied via nanoindentation tests. The effects of loading rates, the maximum load and loading frequency on Young's modulus and the hardness were discussed.

1 Experiment

The preparation of amorphous $Cu_{59}Zr_{36}Ti_5$ and $Cu_{61}Zr_{34}Ti_5$ has been described in our previous work reported elsewhere [14]. The typical procedure is as follows: ingots with the nominal composition of $Cu_{59}Zr_{36}Ti_5$ (sample 1) and $Cu_{61}Zr_{34}Ti_5$ (sample 2) were prepared by arc melting of the highly pure elements under a Ti-gettered argon atmosphere. The ingots were remelted at least 4 times to ensure compositional homogeneity before being cast into cylindrical rods (Φ3 mm in diameter). Then the cylindrical rods were cut into small short rods (6 mm in height) with low speed diamond saw (SYJ 160, China) as specimens used for nanoindentation. All samples were polished to obtain two parallel surfaces of a mirror quality before nanoindentation experiments were carried out on Agilent Nanomechanical Tester G200 fitted with a Berkovitch diamond tip (TB21090) at room temperature. The initial machine calibration was carried out on a fused silica standard specimen.

The details of the tests are as follows: (1) To investigate the effect of loading rates on mechanical response, experiments at the loading rates of 1, 2, 3, 4, 5, 10 and 15 mN/s were conducted to the load limit of 100 mN via CSM mode. (2) To find out the effect of loading frequency on mechanical response, a maximum load of 100 mN was loaded by 5 steps via cycles load control mode at a loading rate of 5 mN/s. The peak load before unloading of each step was the 1/16, 1/8,1/4,1/2 and full of 100 mN. (3) To study the effect of maximum load on mechanical response, the maximum load was controlled via continuous stiffness measurement (CSM) mode to 100, 200, 300, 400, and 500 mN. The loading rate was 5 mN/s, and the unloading rate was the same as the loading rate. For each test, 10 seconds holding period was taken at the peak load before unloading at the same rate of loading rate. At least five indentation tests were carried out randomly for each condition.

2 Results and Discussion

2.1 XRD analysis

Fig.1 shows the XRD patterns of the as cast $Cu_{59}Zr_{36}Ti_5$ and $Cu_{61}Zr_{34}Ti_5$.

As it can be seen from Fig.1, only broad diffraction peaks exist, without any detectable sharp peaks of crystalline phases, indicating the formation of amorphous structure.

2.2 Deformation behavior

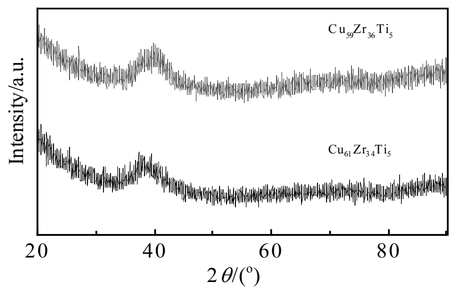

Fig.1 XRD patterns of as cast $Cu_{59}Zr_{36}Ti_5$ and $Cu_{61}Zr_{34}Ti_5$

Fig.2 exhibits the load-displacement curves (ie. *P-h* curves) and the corresponding typical curves obtained from the tests with seven different loading rates. To make it more clear, typical curves are given separately in Fig.2c and 2d. The insert figures highlight the details within the circles.

From Fig.2a and 2b, the experiment data show good repeatability and reproducibility of each tested points under the same experimental conditions, especially when the loading rate is no less than 2 mN/s. Curves obtained from different loading rate show similarity. From Fig.2c and 2d, the curves of total elastic loading stage and the lower elastic-plastic is approximately equal for all seven loading rates. According to Ref.[7,15], solely elastic deformation occurs before the first pop-in. Nevertheless, differences can be observed in the up part of elastic-plastic loading curves. It can be clearly seen that under slow loading rate conditions, obvious serrated flow or pop-in events as marked by arrows can be seen in the loading stage, indicating that shear band events take place in the loading process of the indentation test[16,17]. At the lower loading rate, the pop-in happens. And it's hard to find clear pop-in in the loading curves when the loading rate is higher than 5 mN/s. Interestingly, the loading rate does have an effect on the incipient plasticity. The applied load corresponding to the first pop-in event gradually increases with the increase of loading rate.

Fig.3 shows the load-displacement curves obtained by cyclic loading. Again, to make it more clear, typical curves are given separately in Fig.3c. Although no obvious pop-in is seen in the load-displacement curves, even in the up parts, at the loading rate of 5 mN/s according to Fig.2, serration appearance can be easily found in Fig.3. And after every load cycle, larger load is needed to re-approach the indentation depth at the same location as indicated in Fig.3, meaning hardening happens, especially after the third times reload.

The formation of shear bands is governed by so-called shear transformation zones (STZs), which can be regarded as nuclei for plastic deformation in metallic glasses [18].

During small indentations, the shear field is too small to have sufficient population of STZs and thus shear bands are forced to operate at particular locations leading to increase in hardness[19,20].

Fig.4a shows the typical load-displacement curves of $Cu_{59}Zr_{36}Ti_5$ and $Cu_{61}Zr_{34}Ti_5$ load to different holding loads. To make it more clear, each curves are separated from each other and are shown in Fig.4b.

From Fig.4, no obvious pop-in can be found in the curves of holding load no larger than 300 mN in either alloy. Only slight serration flow behavior can be seen in the load-displacement curves with a holding load of 500 mN. Comparatively speaking, $Cu_{59}Zr_{36}Ti_5$ shows more serration flow behaviors in the loading curve with a holding load of 500 mN, indicating more ability to resist deformation. As mentioned above, the applied load corresponding to the first pop-in event gradually increases with the increase of loading rate. Combining Fig.2 and Fig.4, larger peak load may have the same effects on the serration flow behaviors as slow loading does.

It's suggested that there could be local rise in temperature in regions close to indent-material interface during indentation. The rise in temperature may suffice the energy required to localized melting. This dynamical change of local atomic environments results in pop-in events in load-displacement (i.e. P-h) curves [19]. Larger load may favor the temperature rise close to indent-material interface and lead to serration flow even loaded with high loading rate.

According to the discussion described above, $Cu_{61}Zr_{34}Ti_5$ needs larger load to reach the same depth of indentation as $Cu_{59}Zr_{36}Ti_5$ does, meaning higher resistance to deformation in every test mode. In other words, $Cu_{61}Zr_{34}Ti_5$ is of higher hardness.

2.3 Hardness and Young's modulus

Fig.5 and Table 1 shows the average hardness and Young's modulus of $Cu_{59}Zr_{36}Ti_5$ and $Cu_{61}Zr_{34}Ti_5$ obtained from the load-displacement by different modes. The hardness of each point was calculated at the peak load based on the Oliver–Pharr method [15]. And the modulus of each point was calculated at the initial stage of unloading. As it indicated, the difference between hardness tested by the same mode in this experiment is negligible. In other words, loading rate, value of holding load, and frequency of load has no significant influence on hardness. And the reason may be that the localized deformation regarding to the indented region is similar in structures which is consisted of atomic-scale cluster. However, cyclic loading does show slight hardening for $Cu_{59}Zr_{36}Ti_5$, while $Cu_{61}Zr_{34}Ti_5$ doesn't show such results. It is worth to point out that the modulus of both $Cu_{59}Zr_{36}Ti_5$ and $Cu_{61}Zr_{34}Ti_5$ is sensitive to holding load. The modulus decreases with holding load. And when tested with a loading rate no more

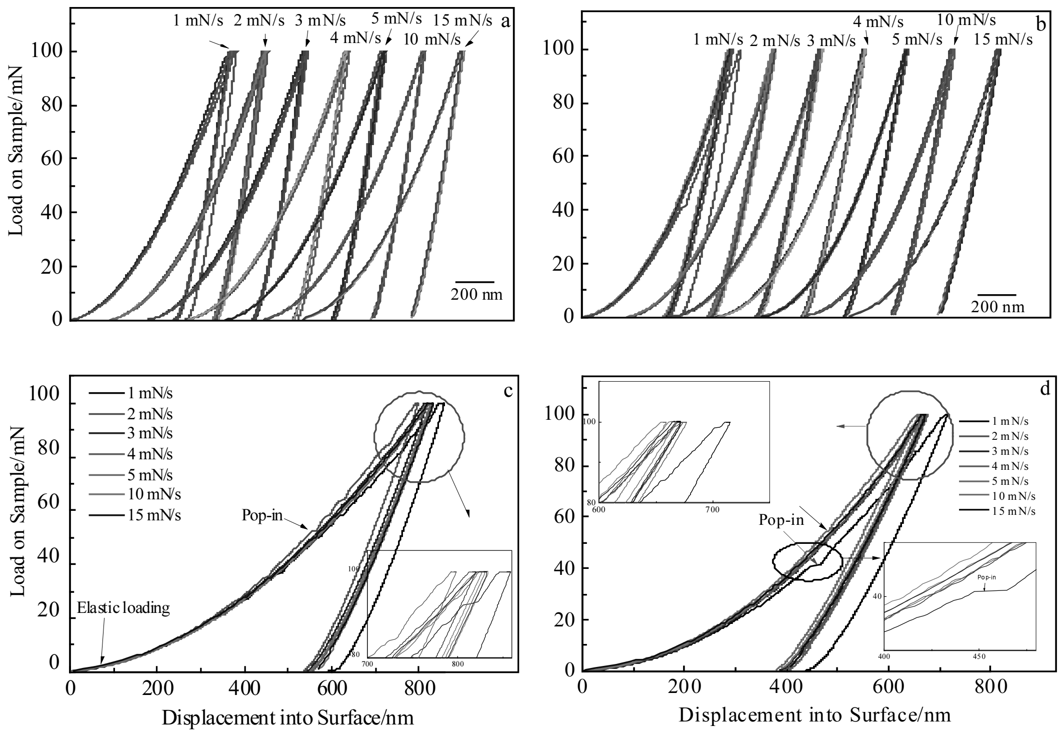

Fig.2 Load-displacement curves and the corresponding typical curves at different loading rates: (a, c) $Cu_{59}Zr_{36}Ti_5$; (b, d) $Cu_{61}Zr_{34}Ti_5$

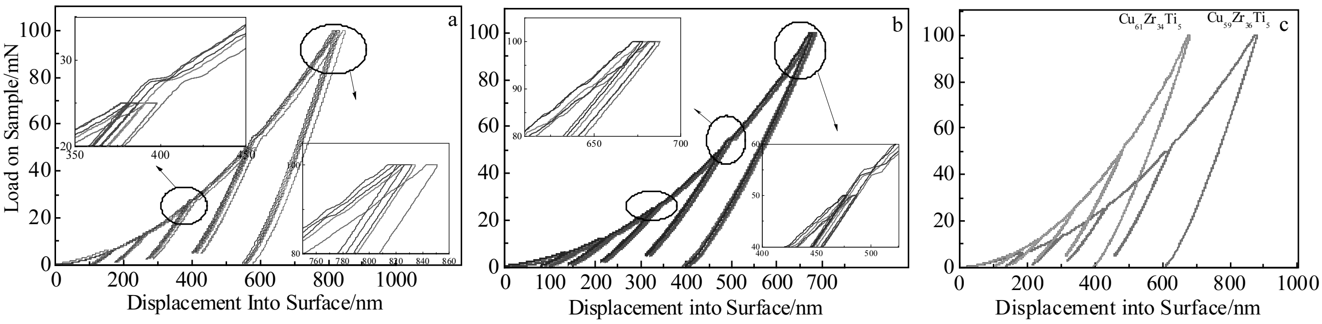

Fig.3 Load-displacement curves of $Cu_{59}Zr_{36}Ti_5$ (a), $Cu_{61}Zr_{34}Ti_5$ (b) and the corresponding typical curves (c) tested by cyclic loading

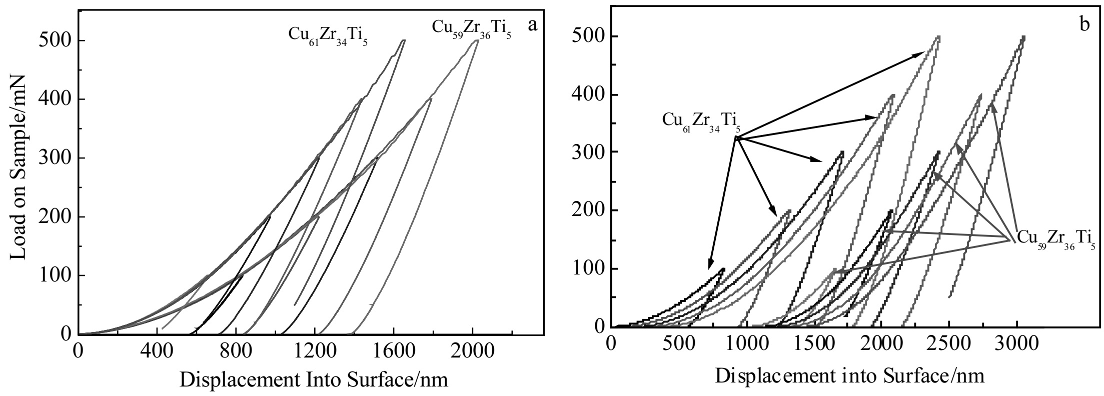

Fig.4 Typical load-displacement curves of different holding loads

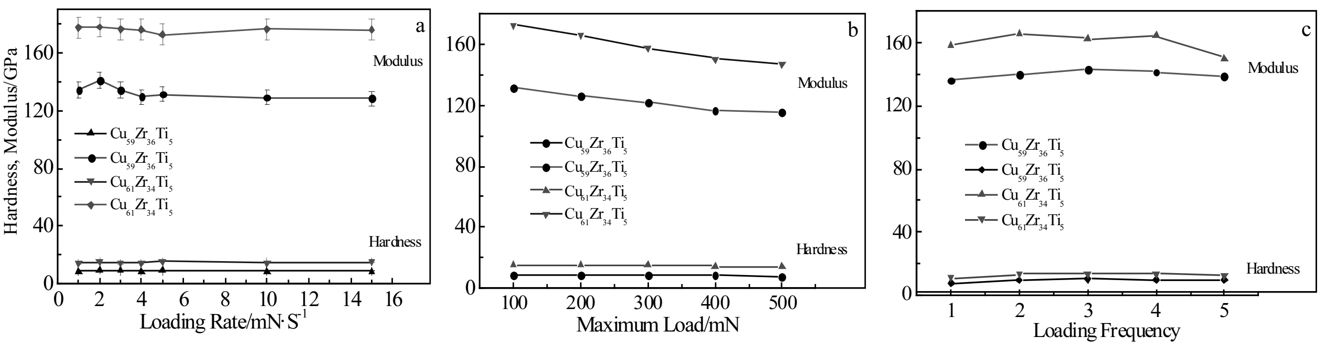

Fig.5 Hardness and Young's modulus of $Cu_{59}Zr_{36}Ti_5$ and $Cu_{61}Zr_{34}Ti_5$ obtained from different loading rate (a), different holding loads (b) and cyclic load (c)

than 5 mN/s, the values of modulus are changing with the loading rate.

It's believed that free volume is enhanced in the region of material affected by the indentation impression. A larger number of net free volume is formed due to high loading rates, causing the coalescence of free volume [9,21]. And the atomic packing will be reduced due to the coalescence of free volume under the indenter, causing the reduction of the reduced modulus (E_r).

Based the method of Oliver and Pharr [15], the hardness is calculated using the following expression:

$$H = \frac{P_{\max}}{A} \tag{1}$$

$$A = \sum_{n=0}^{8} c_n (h_c)^{2-n} = c_0 h^2 + c_1 h + c_2 h^{1/2} + c_3 h^{1/4} + \cdots + c_n h^{1/2^{(n-1)}} + c_8 h^{1/128} \tag{2}$$

Table 1 Average value of hardness and modulus/GPa

Load		$Cu_{59}Zr_{36}Ti_5$		$Cu_{61}Zr_{34}Ti_5$	
		Hardness	Modulus	Hardness	Modulus
Loading rate/mN·s^{-1}	1	8.4	134.4	14.1	177.7
	2	9.0	140.9	14.8	178.1
	3	8.8	134.6	14.3	176.5
	4	8.6	129.6	14.3	176.4
	5	8.8	131.5	15.0	173.0
	10	8.6	129.3	14.5	176.8
	15	8.6	128.5	14.7	176.4
Holding load/GPa	100	8.8	131.5	15.0	173.0
	200	8.4	126.4	15.2	166.3
	300	8.3	121.9	14.8	157.6
	400	7.9	116.6	14.2	150.9
	500	7.7	115.5	13.7	147.6
Loading frequency	1	9.4	140.1	13.1	165.9
	2	10	142.9	13.6	170.8
	3	9.9	141.6	13.2	165.5
	4	9.6	138.8	12.7	165.3
	5	9.3	138.4	12.3	153.4

where, A is the projected contact area and h_c is the contact depth. The Young's modulus of sample can be estimated as follows:

$$\frac{1}{E_r} = \frac{(1-\nu^2)}{E} + \frac{(1-\nu_i^2)}{E_i} \tag{3}$$

$$E_r = \frac{1}{2\beta}\frac{\sqrt{\pi}}{\sqrt{A}}S \tag{4}$$

where, ν is the Poisson's ratio for the specimen, E_i and ν_i are the parameters of the indenter, and β is a constant that depends on the geometry of the indenter (β= 1.034 for a Berkovich indenter). For diamond indenter, E_i=1141 GPa, and ν_i=0.07. S is the contact stiffness, which is calculated from the slope of the initial stage of unloading curve:

$$S = \frac{dP}{dh} \tag{5}$$

It's clear that the reduced modulus takes into account the fact that elastic displacements occur in both the specimen and the indenter. And the reduction of E_r leads to decrease of modulus (E).

Moreover, it is to be observed that $Cu_{61}Zr_{34}Ti_5$ exhibits obviously higher hardness and modulus than $Cu_{59}Zr_{36}Ti_5$ does. It means that the hardness and modulus of copper based bulk metallic glasses are very sensitive to their composition.

3 Conclusions

1) Young's modulus of the specimen shows loading rate dependence when the loading rate is no more than 5 mN/s. The Young's modulus of both $Cu_{59}Zr_{36}Ti_5$ and $Cu_{61}Zr_{34}Ti_5$ decreases with the increasing of holding load and loading frequency.

2) Neither loading rate nor holding load has significant influence on hardness.

3) Cyclic loading leads to slight hardening for $Cu_{59}Zr_{36}Ti_5$, while $Cu_{61}Zr_{34}Ti_5$ doesn't show such results.

4) $Cu_{61}Zr_{34}Ti_5$ exhibits obviously higher hardness and modulus than $Cu_{59}Zr_{36}Ti_5$ does.

References

1 Ma Y, Ye J H, Peng G J *et al*. *Materials Science & Engineering A* [J], 2015, 622: 76
2 Li Fucheng, Ji Gu, Song Min *et al*. *Journal of Alloys and Compounds*[J], 2014, 591: 315
3 Miller M K, Liaw P K. *Bulk Metallic Glasses*[M]. New York: Springer Science+Business Media, 2007
4 Inoue A, Takeuchi A. *Acta Materialia*[J], 2011, 59: 2243
5 Castellero A, Baser T A, Das J *et al*. *Journal of Alloys and Compounds*[J], 2011, 509: 99
6 Fornell J, Pellicer E, Garcia L E *et al*. *Applied Surface Science*[J], 2014, 290: 188
7 Huang Yongjiang, Zhou Binjun, Chiu Yulung *et al*. *Journal of Alloys and Compounds*[J], 2014, 608: 148
8 Kim J T, Hong S H, Lee C H *et al*. *Journal of Alloys and Compounds*[J], 2014, 587: 415
9 Fornell J, Surinach S, Baró M D *et al*. *Journal of Alloys and Compounds*[J], 2011, 509: 87
10 Greer A L, Cheng Y Q, Ma E. *Materials Science and Engineering R*[J], 2013, 74: 71
11 Haag Fabian, Beitelschmidt Denise, Eckert Ju¨rgen *et al*. *Acta Materialia*[J], 2014, 70: 188
12 Wu Jili, Pan Ye, Pi Jinhong. *Appl Phys A*[J], 2014, 115: 305
13 Bhattacharyya Abir, Singh Gaurav, Prasad K Eswar *et al*. *Materials Science & Engineering A*[J], 2015, 625: 245
14 Pan Ye, Zeng Yuqiao, Jing Lijun *et al*. *Materials and Design*[J], 2014, 55: 773
15 Fischer-Cripps A C. *Nanoindentation* [M]. New Yor: Springer, 2011
16 Medeiros B B, Medeiros M M, Fornell J *et al*. *Journal of Non-Crystalline Solids*[J], 2015, 425: 103
17 Huang Yongjiang, Zhou Binjun, Fan Hongbo *et al*. *Materials and Design*[J], 2014, 62: 133
18 Lucca D A, Zare A, Klopfstein M J *et al*. *CIRP Annals-Manufacturing Technology*[J], 2014, 63: 533
19 Vincent S, Murty B S, Kramer M J *et al*. *Materials and Design*[J], 2015, 65: 98

20 Liu Keming, Zhou Haitao, Lu Deping *et al*. *Rare Metal Materials and Engineering*[J], 2010, 39(10): 1732 (in Chinese)

21 Xue Y F, Cai H N, Wang L *et al*. *Composites Science and Technology*[J], 2008, 68(15-16): 3396

铜基块体非晶合金硬度及弹性模量纳米压痕研究

皮锦红，王章忠，贺显聪，白允强

(南京工程学院 江苏省先进结构材料与应用技术重点实验室，江苏 南京 211167)

摘 要：分别采用加载速率控制、载荷控制和循环加载3种不同的纳米压痕模式研究了2种铜基大块金属玻璃$Cu_{59}Zr_{36}Ti_5$和$Cu_{61}Zr_{34}Ti_5$的硬度和弹性模量。当加载速率不超过5 mN/s时，试样的杨氏模量随加载速率而变化。$Cu_{59}Zr_{36}Ti_5$和$Cu_{61}Zr_{34}Ti_5$的弹性模量均随峰值载荷和加载速率的增加而降低。但峰值载荷和加载速率对硬度影响不大。循环加载使$Cu_{59}Zr_{36}Ti_5$产生轻微加工硬化，而$Cu_{61}Zr_{34}Ti_5$则不显示这样的结果。而且，$Cu_{61}Zr_{34}Ti_5$的硬度和模量都明显高于$Cu_{59}Zr_{36}Ti_5$。

关键词：纳米压痕；铜基非晶；循环加载；加工硬化

作者简介：皮锦红，女，1977 年生，博士，副教授，南京工程学院材料工程学院，江苏 南京 211167，电话：025-86118274，E-mail: pijinhong@njit.edu.cn